JCTC Journal of Chemical Theory and Computation

pubs.acs.org/JCTC Article

M11pz: A Nonlocal Meta Functional with Zero Hartree−Fock Exchange and with Broad Accuracy for Chemical Energies and Structures

Siriluk Kanchanakungwankul,[‖] Pragya Verma,*[,‖] Benjamin G. Janesko, Giovanni Scalmani, Michael J. Frisch, and Donald G. Truhlar*

Cite This: *J. Chem. Theory Comput.* 2023, 19, 9102−9117 Read Online

ACCESS | Metrics & More | Article Recommendations | Supporting Information

ABSTRACT: The accuracy of Kohn−Sham density functional theory depends strongly on the approximation to the exchange-correlation functional. In this work, we present a new exchange-correlation functional called M11pz (M11 plus rung-3.5 terms with zero Hartree−Fock exchange) that is built on the M11plus functional with the goal of using its rung-3.5 terms without a Hartree−Fock exchange term, especially to improve the accuracy for strongly correlated systems. The M11pz functional is optimized with the same local and rung-3.5 ingredients that are used in M11plus but without any percentage of Hartree−Fock exchange. The performance of M11pz is compared with eight local functionals, and M11pz is found to be in top three when the errors or ranks are averaged over eight grouped and partially overlapping databases: AME418/22, atomic and molecular energies; MGBE172, main-group bond energies; TMBE40, transition-metal bond energies; SR309, single-reference systems; MR54, multireference systems; BH192, barrier heights; NC579, noncovalent interaction energies; and MS20, molecular structures. For calculations of band gaps of solids, M11pz is the second best of the nine tested functionals that have zero Hartree−Fock exchange.

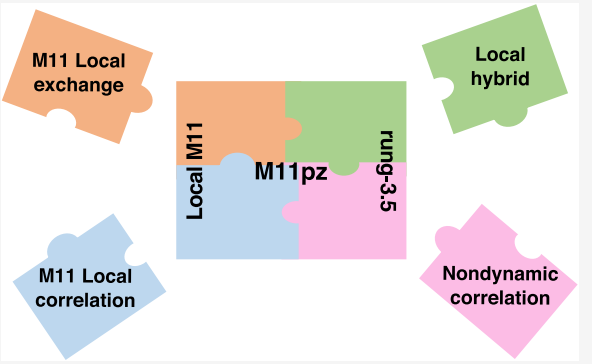

1. INTRODUCTION

Kohn−Sham density functional theory[1,2] is the most widely used quantum mechanical electronic structure method for molecules and materials.[3] The key to the success of density functional calculations lies in the accuracy of the necessarily approximate exchange−correlation functionals; however, the best currently available density functionals suffer from self-interaction error and delocalization error.[4,5] Therefore, the development of better approximate exchange−correlation functionals is a major goal in theoretical chemistry. One route to improving functionals is to add new ingredients.[6] The simplest exchange−correlation functionals are local functionals in which the energy density at a point in space depends only on local properties such as the local spin densities (ρ_σ, where σ is α or β), their reduced gradients defined as

$$s_\sigma = |\nabla\rho_\sigma|/[2(6\pi^2)^{1/3}\rho_\sigma^{4/3}]$$

in the spin-polarized form (see Appendix A of ref 7), and the local kinetic energy densities (τ_σ). Functionals for which the energy density at a point in space involves an integral over the entire space are called nonlocal. The most popular nonlocal functionals are called global hybrids; in these, a portion[8] (or sometimes all) of the local exchange is replaced by a percentage (denoted X) of nonlocal Hartree−Fock (HF) exchange; in these functionals, X is independent of the interelectronic distances. Other types of nonlocal functionals containing HF terms are range-separated hybrids[9] and local hybrids[10,11] (LHs) in which X can vary with interelectronic separation or other variables. Hybrid functionals decrease self-interaction error and delocalization error, often leading to more accurate thermochemistry, chemical reaction barrier heights, and excitation energies.[3,7,8,12−14] However, nonzero X can also make the functional less accurate for systems that have large static correlation (called strongly correlated systems or multireference systems), like many molecules containing transition metals,[15,16] and in some implementations (especially those employing plane wave codes), it can appreciably raise the computational cost.

Local functionals account for static correlation through the local exchange terms. A type of functional that attempts to model static correlation more accurately has nonlocal ingredients called rung-3.5 terms. Rung-3.5 terms involve the

Received: December 29, 2022
Published: December 14, 2023

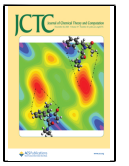

https://doi.org/10.1021/acs.jctc.2c01315
J. Chem. Theory Comput. 2023, 19, 9102−9117

expectation value of range-restricted nonlocal one-electron operators that sample the off-diagonal part of the one-particle reduced density matrix. An adiabatic-projection derivation of rung-3.5 density functionals that shows their relation to self-interaction corrections and Hubbard corrections has been presented elsewhere.[17] Previously, we developed a novel functional called M11plus[18] that combines M11 local exchange & correlation terms,[19] HF exchange terms (in a range-separated hybrid form), and rung-3.5 terms. The local terms and HF terms in M11plus have the same functional form as those employed in a previous range-separated-hybrid meta-generalized gradient approximation called M11.[19] After addition of the new rung 3.5 ingredient to the M11 functional, the parameters were re-optimized to obtain M11plus. The M11plus functional has been found to have broad accuracy with especially good improvement on strongly correlated systems. This improvement can be ascribed to the new rung-3.5 terms that were added to the M11 functional form to explicitly account for the nondynamic (static) correlation in the exchange−correlation functional.

The new functional presented here consists of M11 local exchange and M11 local correlation (which have ingredients that depend on spin densities, reduced spin-density gradients, and kinetic energy densities) and rung-3.5 nonlocal correlation, all of which are also present in M11plus, but it differs from M11plus in not having HF exchange (it has $X = 0$) and in having the other parameters reoptimized. Therefore, the new functional form is equivalent to M11plus with zero Hartree−Fock exchange, and for brevity we name it M11pz, where the "p" is short for "plus" and the "z" is short for "zero Hartree−Fock exchange."

The exchange−correlation energy is given by

$$E^{\mathrm{M11pz}} = E^{\mathrm{M11x}} + E^{\mathrm{M11c}} + E^{3.5} \tag{1}$$

where the first term has the form of M11 local exchange

$$E^{\mathrm{M11x}} = E^{\mathrm{M11x}}(\rho_\alpha, \rho_\beta, s_\alpha, s_\beta, \tau_\alpha, \tau_\beta) \tag{2}$$

the second term has the form of M11 local correlation

$$E^{\mathrm{M11c}} = E^{\mathrm{M11c}}(\rho_\alpha, \rho_\beta, s_\alpha, s_\beta, \tau_\alpha, \tau_\beta) \tag{3}$$

and the third term equals the sum of two kinds of rung-3.5 correlation terms

$$E^{3.5} = \sum_\sigma E_\sigma^{\mathrm{LH}} + E^{\mathrm{B05}} \tag{4}$$

The local terms in M11pz are described in the M11 paper,[19] and the rung-3.5 terms have the same form as those in the M11plus functional and are presented in complete detail in the M11plus paper.[18] There are two kinds of rung-3.5 terms in M11plus and M11pz: E_σ^{LH} is an energy term motivated by local hybrid theory[10,11] and E^{B05} is an energy term based on Becke's 2005 nondynamic correlation functional[20] (details are in ref 18). Note that although the functional forms are the same as presented previously, the linear parameters are re-optimized, as discussed below.

There is more than one motivation for developing a new functional with zero HF exchange. First, turning off nonlocal HF exchange reduces the computational cost for plane-wave calculations;[21,22] the actual speedup depends on the particular code and other parameters, but in our experience, it is often 2−3 orders of magnitude. Another motivation is that long-range HF exchange (in global hybrids or long-range-corrected hybrids) causes a divergence of the group velocity at the Fermi level for solid-state systems (like metals) that do not have a gap.[23,24] A third motivation, perhaps the most important of all, is that HF exchange causes static correlation error,[25] and static correlation error is generally somewhat smaller when HF exchange is not present. However, due to greater self-interaction error, functionals with zero HF exchange tend to show less accuracy than functionals with HF exchange for many problems not dominated by static correlation error.

The new M11pz functional is not local because it contains the nonlocal rung-3.5 correlation terms of eq 4, but it is not hybrid because "hybrid" in the density functional literature has the generally accepted meaning of referring to the inclusion of some HF exchange. It will be convenient to have a simple way to refer to functionals with zero HF exchange, and we will use the term "nonhybrid" for that.

2. DATABASE AND METHODOLOGY

2.1. Databases. We begin with Minnesota Database 2019 (MDB 2019),[26,27] which is a collection of databases containing both experimental data and high-quality theoretical data. We made a few minor changes to this database, as explained below. The revised database is named Minnesota Database 2019/22, but in the rest of this article we simply refer to the revised database as MDB.

The MDB has data for both single-reference (SR) and multireference (MR) systems; SR and MR systems are also called weakly correlated and strongly correlated systems, respectively. The correlation energy of weakly correlated systems is mainly or entirely dynamic, whereas that of strongly correlated systems also contains a significant amount of static correlation (which is due to near-degeneracy effects and is also called nondynamic correlation). It is well appreciated that Kohn−Sham density functional theory is more accurate for dynamic correlation than for static correlation.[3,25,28−30] The inclusion of significant MR data is very appropriate for optimizing M11plus and M11pz since they contain rung-3.5 terms that should provide a better description of static correlation than density functionals with only more conventional ingredients.

A subset, shown in Table 1, of MDB is used for training the M11pz functional, and the databases in this subset are also used for testing against selected other functionals. Thus, they are called training-and-testing databases since they are used for both purposes. These are mainly the same databases as were used in M11plus functional optimization, and references are given in Table 2 of ref 26. The differences from refs 18 (M11plus) and 26 (revM11) are that we added the LC18 database and 37 repulsive energies from the PEC150 database in the training set for the optimization of M11pz, and we made some minor changes that are explained in the footnotes of Table 1. The LC18[31] database has 18 lattice constants for 17 solids, and it was previously called LC17.[32] The PEC150 database consists of potential energy curves of five van der Waals complexes (Ne_2, Ar_2, Kr_2, KrHe, and benzene···Ar[33]) of which four (Ne_2, Ar_2, Kr_2, and KrHe) are from the testing set of our previous work (PEC4 in revM11[26] and M11plus[18]), and the benzene···Ar complex[33] is newly added in this work. For the four inert gas dimers in PEC4, we used 36 interatomic distances for Ne_2, 31 interatomic distances for Ar_2, 31 interatomic distances for Kr_2, and 31 interatomic distances for KrHe, which altogether total 129 energy points; therefore, we renamed PEC4 as PEC129 in the present work because we are moving to a naming convention where the number in the database name always (rather than just usually) gives the

https://doi.org/10.1021/acs.jctc.2c01315
J. Chem. Theory Comput. 2023, 19, 9102−9117

Table 1. Databases Used for Training and Testing

database[a]	description	inverse weight[b]
SR-MGM-BE8	single-reference main-group metal bond energies	0.90
SR-MGN-BE107	single-reference main-group nonmetal bond energies	0.045
SR-TM-BE15	single-reference transition-metal bond energies	0.60
MR-MGM-BE4	multireference main-group metal bond energies	0.11
MR-MGN-BE17	multireference main-group nonmetal bond energies	3.00
MR-TM-BE13[c]	multireference transition-metal bond energies	0.03
MR-TMD-BE3	multireference transition-metal dimer bond energies	1.00
HTBH38/18	hydrogen-transfer barrier heights	0.10
NHTBH38/18	non-hydrogen-transfer barrier heights	0.075
NCCE23/18	noncovalent complexation energies	0.04
CT7/04	noncovalent complexation energies (charge transfer)	0.04
NGD21/18	noble gas dimer weak interactions	0.01
S6x6	noncovalent interaction energies of six dimers at six intermonomer distances (subset of S66x8)	0.015
IP23	ionization potentials	0.12
EA13/03	electron affinities	0.14
PA8	proton affinities	0.13
pBIsoE8[d]	2p- and 4p-block isomerization energies	40.00
IsoL6/11	isomerization energies of large molecules	20.00
πTC13	thermochemistry of π systems	[e]
AE17	atomic energies	0.17
HC7/11	hydrocarbon chemistry	0.42
SMAE3/19	sulfur molecule atomization energies	2.00
DC9/19	difficult cases	0.18
ABDE13	alkyl bond dissociation energies	40.00
DGL6	diatomic geometries (bond lengths) for diatoms with light atoms	0.009
DGH4	diatomic geometries (bond lengths) for diatoms with one or more heavy atom	0.009
3dEE7/22[f]	excitation energies of 3d transition-metal atoms and Fe_2	0.08
4dAEE5	4d transition-metal atomic excitation energies	0.45
pAEE5	p-block atomic excitation energies	0.20
LC18	lattice constants of solids	0.004
PEC37[g]	37 repulsive energy points from the potential energy curves of Ne_2, Ar_2, Kr_2, KrHe, and benzene···Ar	0.004

[a]The number of data is given by the number ending the database name if there is no solidus and by the number before the solidus when it is present. The references for all of the databases are provided in ref 26, except for the LC18 database, benzene···Ar (in the PEC37 and PEC150 databases), and FeO^+ (in the MR-TM-BE13 database), where LC18 is provided in ref 31 and the latter two are provided in this work. [b]Inverse weight is the reciprocal of the weight used with each database during optimization of the functional as explained in eq 5 in Section 2.3. All inverse weights are in kcal/mol or Å. [c]MR-TM-BE13 adds the bond energy of FeO^+ into MR-TM-BE12. [d]pBIsoE8 is the merger of databases 2pIsoE4 and 4pIsoE4. [e]During optimization, πTC13 database was treated as two subdatabases (πIE3 and πPA10) with different inverse weights, 2.50 and 0.20, respectively. [f]3dEE7/22 excludes Ca^+ from 3dEE8. [g]PEC150 adds 21 energy points of benzene···Ar to database PEC129 (formerly called PEC4 in ref 26), which contains 129 energy points. The 37 points of PEC150 that are in repulsive regions were used for training and testing, and the remaining points were used only for testing.

number of data points. After adding 21 intermonomer distances of benzene···Ar, the database then has 150 energy points, which we call PEC150. The PEC150 database has 37 of the 150 energy points in repulsive regions of the five complexes, and only these 37 were used for training.

The basis sets used for most of the databases except benzene···Ar (in the PEC150 database) and FeO^+ (in the MR-TM-BE13 database), are described in earlier work, for example, most of molecular databases are in ref 26, and most of the solid-state databases are in ref 7.

For benzene···Ar, the reference values for each of the 21 points on the potential energy curve are calculated using the CCSD(T) method[34] and the aug-cc-pVQZ basis set.[35−37] Its equilibrium geometry is obtained from the Supporting Information of ref 33. The density functional calculations for benzene···Ar also used the aug-cc-pVQZ basis set.

For FeO^+, the calculation of bond energy is done using the aug-cc-pVTZ basis set[35,36] for triplet O and the aug-cc-pwCVTZ basis set[38] for sextet Fe^+. The ground spin state of FeO^+ is a sextet state. The equilibrium bond length (r_e) of FeO^+ is 1.638 Å estimated from an experimental r_0.[39,40] The reference spin-orbit-free equilibrium bond energy, D_e, of FeO^+ is calculated to be 83.8 ± 0.5 kcal/mol. We obtained this from the experimental zero-point dissociation energy (D_0 = 81.2 ± 0.5 kcal/mol)[41] by removing zero-point energy and spin-orbit coupling. The zero-point energy was estimated in the harmonic approximation as 1.20 kcal/mol based on the experimental[42] fundamental frequency. The spin−orbit energies were obtained from atomic energy levels in the NIST database as −1.19 kcal/mol for Fe^+ and −0.22 kcal/mol for O (the spin-orbit energy of FeO^+ is zero because it is a Σ state).

The performance of the M11pz functional is further evaluated on testing databases that are listed in Table 2. Some of these testing databases are from MDB 2019, as described in Table 3 of ref 26. Those not in MDB include both molecular and solid-state databases. The molecular databases not in MDB are (i) four databases from GMTKN55,[43] namely, ALKBDE10, WCPT18, W4-11, and RSE43, which were also used in the assessment of the M11plus functional[18] and (ii) a database with 41 metal−organic reactions (MOR41).[44] The solid-state databases contain transition-metal oxide band gaps (TMOBG4)[45] and semiconductor band gaps (SBG31).[7] More explanations of the databases are in the footnotes of Table 2 and references in the footnotes of Table 2.

2.2. Computational Details. For selected databases, the errors for the new M11pz functional were compared to those for 15 other functionals, including eight local functionals (BLYP,[50,51] PBE,[52] OreLYP,[51,53,54] GAM,[55] TPSS,[56] M06-L,[57] MN15-L,[58] and revM06-L[32]) and seven nonlocal functionals (B3LYP,[50,51,59,60] B97-1,[61] PW6B95,[62] PW6B95-D3(BJ),[62,63] MN15,[64] revM06,[65] and M11plus[18]). For all the databases, the errors for M11pz were compared to those for the eight local functionals.

The M11pz functional was optimized using *Gaussian Development Version, Revision J.16*,[66] and *Gaussian Development Version, Revision I.14+* [67] was used for calculations with M11plus. Calculations for BLYP, PBE, TPSS, M06-L, MN15-L, B3LYP, B97-1, PW6B95, PW6B95-D3(BJ), and MN15 were performed using *Gaussian 16*;[68] calculations for GAM, revM06-L, and revM06 were performed using a locally modified version of *Gaussian 16*; and calculations for OreLYP were performed with *Minnesota-Gaussian Functional Module* (*MN-GFM6.10*).[69] All calculations were done using the UltraFine grid (99, 590

https://doi.org/10.1021/acs.jctc.2c01315
J. Chem. Theory Comput. 2023, 19, 9102−9117

Table 2. Databases Used Only for Testing

database[a]	description
	Databases in MDB
AL2X6	dimerization energies of aluminum compounds
ASNC2	atmospheric sulfur−nitrogen cluster binding energies
BHDIV10	barrier heights of diverse reactions
BHPERI26	barrier heights of pericyclic reactions
BHROT27	barrier heights for rotation around single bonds
DIPCS10	double-ionization potentials of closed-shell systems
DM79	dipole moments (ground state)
HeavySB11	dissociation energies of heavy-element compounds
PX13	proton-exchange barriers of H_2O, NH_3, and HF clusters
SIE4x4	self-interaction errors
S66x8	noncovalent interaction energies of complexes relevant to biomolecules
YBDE18	ylide bond-dissociation energies
TMBH22	transition-metal reaction barrier heights of Mo, W, Zr, and Re reactions
TMDBL10	transition-metal dimer bond lengths
WCCR9/18[b]	ligand dissociation energies of large cationic transition-metal complexes
PEC150[c]	potential energy curves of five dimers—Ne_2, Ar_2, Kr_2, KrHe, and benzene···Ar
	Databases not in MDB
ALKBDE10[d]	dissociation energies of group-1 and group-2 diatomics
RSE43[d]	radical stabilization energies
WCPT18[d]	proton-transfer barriers of uncatalyzed and water-catalyzed reactions
W4-11[d]	total atomization energies
MOR41[d,e]	metal−organic reactions
TMOBG4[f]	transition-metal oxide band gaps
SBG31[g]	semiconductor band gaps

[a]When not stated otherwise, the number of data is given by the number ending the database name if there is no solidus and by the number before the solidus when it is present. Some of these testing databases are from MDB 2019, as described in Table 3 of ref 26. Those not in MDB include both molecular and solid-state databases, as described in the text of the present paper. [b]WCCR9/18 is from WCCR10/18 by excluding reaction 4 from ref 46. [c]As mentioned in footnote *g* of Table 1, 37 of these data were used for training and testing, and the remaining data were used only for testing. [d]The molecular databases not in MDB consist of five databases (ALKBDE10, RSE43, WCPT18, W4-11, and MOR41) of which the first four are from GMTKN55; they used the def2-QZVP basis set, and the geometries of systems in each database are described in ref 43. [e]The MOR41 database used the def2-QZVP basis set, and the geometries and reference values are from ref 44. [f]The TMOBG4 database used the POB-TZVP[47] basis set with reference values in the Supporting Information of ref 48. [g]The 31 semiconductor band gaps database (SBG31) used three sets of basis set explained in refs 48 and 49, and the geometries and reference values are also from those references and references therein.

grid), which is a pruned grid having 99 radial shells and 590 angular points per shell.

All databases except DGL6, DGH4, TMDBL10, and LC18 involve single-point calculations at geometries specified as part of the database. For the calculation of geometrical parameters with units of length in bond-length databases (DGL6, DGH4, and TMDBL10) and in the lattice-constant database (LC18), energy calculations were performed at at least five bond distances or seven lattice constants, and equilibrium bond lengths and lattice constants were obtained from least-squares fitting to these energies.

Stability checks were performed for all calculations on the ground-state and the three excited-state (3dEE7/22, 4dAEE5, and pAEE5) databases, but not for the solid-state databases—lattice constants database (LC18), semiconductor band gaps database (SBG31), and transition-metal oxide band gaps database (TMOBG4). Electronic excitation energies for the three excited-state databases were calculated by the ΔSCF method.

Some data include zero-point vibrational energy, spin−orbit coupling, and scalar relativistic effects. These details are explained in the revM11 paper.[26]

2.3. Functional Optimization. The M11pz functional form is obtained from that of M11plus by eliminating its HF exchange. The functional forms of the local exchange and local correlation terms in M11plus (and hence in the new functional presented here) are the same as in M11.[19] During optimization of M11pz, the linear parameters of the M11 local exchange and M11 local correlation and of the M11plus rung-3.5 terms were optimized using the training databases of Table 1. The nonlinear parameters of the rung-3.5 terms (eq 4) are fixed to be the same as in the M11plus functional (as given in Table 1 of ref 18). In particular, the optimization of M11pz involves 36 linear coefficients—combining 28 from local M11 terms and eight from rung-3.5 terms (four from local-hybrid terms + four from B05 terms). These coefficients were optimized to minimize the following function

$$F = \sum_{n=1}^{31} \frac{R_n}{I_n} + \lambda(a^x + b^x + a^c + b^c) \tag{5}$$

where the sum is over the 31 databases in Table 1, R_n is the root-mean-square error (RMSE) of database n defined by

$$R_n = \sqrt{\frac{1}{m}\sum_{i=1}^{m}(x_{\mathrm{cal},i} - x_{\mathrm{ref},i})^2} \tag{6}$$

where m defines the number of data points in each database n; $x_{\mathrm{cal},i}$ and $x_{\mathrm{ref},i}$ are the calculated and reference values, respectively, of datum i in database n; I_n is the inverse weight assigned to each database; λ is the smoothness restraint parameter; and the terms multiplied by λ are given by

$$a^x = \sum_{i=0}^{5}(a_i^x - a_{i+1}^x)^2$$
$$b^x = \sum_{i=0}^{5}(b_i^x - b_{i+1}^x)^2$$
$$a^c = \sum_{i=0}^{5}(a_i^c - a_{i+1}^c)^2$$
$$b^c = \sum_{i=0}^{5}(b_i^c - b_{i+1}^c)^2 \tag{7}$$

where a_i^x and b_i^x are the linear coefficients of the local exchange and a_i^c and b_i^c are the linear coefficients of the local correlation terms of the M11 component in M11pz. The smoothness restraint parameter λ is set equal to 0.02, which is the same as used in optimizing the M11plus and revM11 functionals. A higher λ provides higher functional smoothness, but it is found to worsen the performance of the M11pz functional on the calculation of some of the databases. Therefore, we decided to

https://doi.org/10.1021/acs.jctc.2c01315
J. Chem. Theory Comput. 2023, 19, 9102−9117

Table 3. Optimized Linear Coefficients of M11pz

M11 local components			rung-3.5 components			
coeff.	exchange	correlation	coeff.	LH	coeff.	B05
a_0	1.779814645	0.654261662	c_0	−0.075495695		
a_1	−10.571375988	−0.207847301	c_1	−0.214440400	d_1	−0.529686873
a_2	1.629528796	6.103621816	c_2		d_2	0.304731639
a_3	8.197709995	−8.341650131	c_3	3.125017527	d_3	0.574245383
a_4	1.367809302	−16.74138168	c_4	−2.904680019	d_4	0.527981900
a_5	6.989993689	2.670647007				
a_6	−1.721874988	15.009114025				
b_0	−0.734882925	1.346551698				
b_1	10.968372186	−4.895049845				
b_2	−2.562767164	−9.335618679				
b_3	−7.450063720	−11.261291120				
b_4	−0.833616768	−1.119367653				
b_5	−8.134636163	−15.895534350				
b_6	2.075989103	−17.83586876				

use the same λ of 0.02 to balance the smoothness and the accuracy of the functional. The summation term in eq 5 minimizes the RMSE in reproducing the reference data and the λ terms promote smoothness in the functional. For the other eight linear parameters from rung-3.5 terms, we did not use the smoothness restraint.

The final functional obtained by this process depends strongly on the inverse weights I_n used with the databases (see eq 5), and that is where the optimization becomes an art rather than a science. The use of inverse weights has the slight disadvantage that the reader must keep in mind that a large inverse weight means a lower importance in the fitting, but they have the major advantage that the inverse weight has the same units as the property in question, and its magnitude shows the relative sought accuracy for that property. The optimization involves many rounds of changing the inverse weights to get good across-the-board accuracy. This means we want small errors on every database, but if we must make the inverse weight of some database so small that the errors on other databases rise too rapidly, then we make the decision to accept larger errors for the databases in question. The first round of inverse weights is chosen based mainly on errors obtained with electron densities from a previous functional, but then the densities are updated with self-consistent field calculations employing the new functional. The new densities lead to new calculations of all of the terms contributing to the energies, for all data in the training set, and a new choice of inverse weights is made based on this new data; this leads via eq 5 to new round of coefficients and hence another new functional, leading to newer densities, leading to new weights, until the process does not seem to allow for further improvement. At that point, the parameters are finalized. The final linear coefficients of M11pz are given in Table 3.

2.4. Statistical Analysis. No single statistic can fully capture performance, and this is especially true when one seeks to compare methods (in our case, density functionals) over diverse databases with non-normal error distributions; variable number of data; and different magnitudes of the data, the data errors, and the percentage errors of the data. Some of the data even have different units. Since no error measure will fully capture quality and universality of the functionals under examination, but some measure of this is needed for capturing trends, and since avoiding complicated weighting schemes makes the analysis easier to comprehend, we chose the following simple scheme to compare the performance of functionals.

On a given database, the metric used is mean unsigned error (MUE), which is given by

$$\mathrm{MUE} = \frac{1}{m}\sum_{i=1}^{m} |x_{\mathrm{cal},i} - x_{\mathrm{ref},i}| \tag{8}$$

where m is the number of data in the evaluation, $x_{\mathrm{cal},i}$ is the calculated value, and $x_{\mathrm{ref},i}$ is the reference value (experimental value or high-level theory as specified in the database). We use MUE because it is a simple, robust quality indicator for distributions that do not necessarily have a normal error distribution, and its use on the smaller databases where the data are more homogeneous in character is reasonable. But to compare the performance of functionals across several databases that are quite different from each other, we use average rank. That is, for each of the individual databases, we rank all of the functionals in order of MUE (the lowest MUE gets rank 1, the second lowest rank 2, and so forth). Then, we compute the average rank of each functional over a set of databases. In later discussions, we also report overall MUE of combined databases that we obtain by grouping several databases together. The overall MUE can be calculated as

$$\text{overall MUE} = \frac{\sum_i^n (m_i \times \mathrm{MUE}_i)}{\sum_i^n m_i} \tag{9}$$

where i is the index of summation representing a database, n is the number of databases, m_i is the number of data in database i, and MUE_i is the mean unsigned error of each database i.

We also examine the performance of functionals using the maximum absolute error of each functional on each database. The maximum absolute error of a given database is the largest error calculated from the absolute difference between calculated values and reference values. We also ranked the functionals by the maximum absolute error on the databases, where the lowest maximum absolute error gets rank 1, the second lowest rank 2, and so forth.

3. RESULTS AND DISCUSSION

The MUEs of 29 of the training-and-testing databases calculated by local and nonlocal functionals are shown in Table 4. (The LC18 training-and-testing database and the PEC150 database,

https://doi.org/10.1021/acs.jctc.2c01315
J. Chem. Theory Comput. 2023, 19, 9102−9117

Table 4. Mean Unsigned Errors (MUEs) of 16 Functionals for 29 of the Training-and-Testing Databases

database	B3LYP	B97-1	PW6B95-D3(BJ)	PW6B95	MN15	revM06	M11plus	BLYP	PBE	OreLYP	GAM	TPSS	M06-L	MN15-L	revM06-L	M11pz
MUEs of Ground-State Energies (kcal/mol)																
SR-MGM-BE8	4.4	2.2	2.4	2.1	1.6	1.8	2.6	4.9	2.5	4.3	2.1	3.0	3.8	2.6	2.5	3.6
SR-MGN-BE107	2.2	1.5	1.1	1.1	0.9	1.0	1.0	2.6	3.4	2.6	2.3	2.3	2.0	1.5	1.8	1.9
SR-TM-BE15	4.4	3.1	2.6	1.9	2.9	2.8	4.6	4.8	5.4	5.7	4.5	4.0	4.4	3.0	5.4	4.0
MR-MGM-BE4	7.8	6.0	7.6	7.4	3.9	6.4	6.9	8.7	9.3	8.3	7.8	6.7	11.9	1.9	6.4	6.8
MR-MGN-BE17	5.1	3.2	4.7	3.4	2.8	4.2	5.4	6.7	12.1	4.2	4.2	4.2	3.0	2.1	2.3	2.7
MR-TM-BE13	4.6	2.8	4.9	4.6	3.9	6.3	5.6	11.4	11.5	6.3	5.6	7.3	4.7	3.8	4.1	2.9
IsoL6/11	2.6	1.8	2.0	1.7	1.8	1.0	2.4	3.7	2.0	3.4	2.0	3.7	2.8	1.3	1.3	1.8
IP23	5.3	2.5	2.9	3.1	2.5	3.1	3.1	6.4	6.0	2.8	4.4	4.1	3.9	2.5	4.5	3.6
EA13/03	2.3	2.0	1.8	1.8	0.9	1.6	1.4	2.7	2.2	2.3	4.4	2.3	3.8	2.1	5.4	1.9
PA8	1.0	1.6	1.2	1.2	1.1	1.6	2.0	1.6	1.3	1.7	3.8	2.7	1.9	2.2	2.6	2.6
πTC13	6.0	7.0	5.8	5.9	3.5	2.8	1.8	6.1	5.6	7.3	8.6	8.1	6.7	4.8	7.0	6.6
HTBH38/08	4.5	4.8	3.5	3.8	1.1	1.5	1.0	7.9	9.7	6.7	5.8	8.1	4.6	1.3	2.0	3.5
NHTBH38/08	4.5	3.3	2.8	2.9	1.7	1.1	1.3	8.5	8.4	5.6	5.1	8.9	3.7	2.0	2.2	2.9
NCCE23/18	1.43	0.78	0.65	0.50	0.39	0.34	0.47	1.96	0.97	3.49	0.68	1.19	0.31	0.81	0.47	0.48
CT7/04	0.65	1.14	0.64	0.99	0.37	0.53	0.69	1.62	2.93	1.45	2.69	2.18	1.74	0.80	1.08	1.55
AE17	18.3	5.4	98.6	98.6	6.8	3.9	5.8	8.4	47.3	2.4	10.2	18.1	7.0	7.5	4.5	6.5
HC7/11	16.8	6.3	4.1	2.3	3.7	2.4	5.4	27.4	4.0	16.3	6.2	10.5	3.4	4.0	3.5	3.0
DC9/19	6.2	4.9	3.5	2.9	2.3	1.8	1.7	8.2	6.5	8.2	6.6	6.2	3.7	2.8	2.7	2.7
pBIsoE8	4.5	2.7	2.0	1.8	1.1	2.2	1.3	4.7	2.6	3.0	4.3	3.1	3.0	2.9	5.1	4.7
NGD21/18	0.28	0.08	0.12	0.08	0.02	0.04	0.05	0.38	0.10	0.39	0.02	0.17	0.13	0.02	0.07	0.06
MR-TMD-BE3	27.8	23.2	66.4	34.0	22.8	43.5	15.9	31.4	18.7	8.9	10.6	12.3	6.5	20.9	20.8	11.5
S6x6	3.78	2.45	1.93	0.24	0.34	0.55	0.61	4.96	2.61	8.23	1.68	3.52	0.80	1.72	0.79	0.72
SMAE3/19	3.5	1.1	1.7	2.0	0.1	0.8	0.8	1.4	4.4	1.0	1.3	2.0	1.1	1.1	1.2	1.3
ABDE13	8.6	3.5	2.7	1.8	1.8	1.3	1.3	12.0	5.1	10.8	6.3	10.7	5.3	4.6	2.4	6.0
MUEs of Ground-State Bond Lengths (Å)																
DGL6	0.009	0.006	0.004	0.007	0.005	0.008	0.009	0.019	0.013	0.011	0.007	0.010	0.006	0.004	0.009	0.005
DGH4	0.028	0.027	0.015	0.015	0.011	0.018	0.017	0.040	0.021	0.034	0.036	0.014	0.009	0.024	0.009	0.015
MUEs of Excitation Energies Calculated by ΔSCF Method (kcal/mol)																
3dEE7/22	9.1	8.1	8.2	8.7	8.5	7.4	7.2	12.7	8.1	12.0	8.7	8.6	5.0	2.5	7.0	7.0
4dAEE5	6.3	6.7	5.4	5.4	5.9	3.9	6.6	6.3	5.3	5.8	4.6	5.8	7.2	1.1	5.0	4.5
pAEE5	2.6	2.5	1.8	1.8	4.5	4.5	3.5	4.9	3.7	3.1	3.2	2.0	7.7	5.0	7.3	5.3

https://doi.org/10.1021/acs.jctc.2c01315
J. Chem. Theory Comput. 2023, 19, 9102−9117

part of which is used for training and testing (PEC37) and the rest of which is used only for testing, are not considered in this table but are considered later.) There are three main groups of results in Table 4: ground-state energies, ground-state bond lengths (geometries), and electronic excitation energies calculated by the ΔSCF method. The ΔSCF method consists of calculating the energies of ground and excited states by separate SCF calculations and then taking their difference; ordinarily, this can only be applied when the excited state has a different symmetry than the ground state.

To evaluate the performance of the functionals, the overall MUEs and the average ranks are calculated and shown in Table 5. The final rank in Table 5 is assigned based on average rank rather than overall MUE. Ranks of all functionals based on their MUEs on 29 of the training-and-testing databases are given in Tables S1−S3 (tables with the prefix S are in the Supporting Information).

Table 5. Overall Mean Unsigned Errors (MUEs) and Ranks of the 16 Functionals Based on the 29 Databases of Table 4[a]

functional	overall energetic MUE (kcal/mol)	overall geometric MUE (Å)	average rank	rank of nonhybrid functionals[b]
MN15	1.9	0.007	3.9	NA[c]
revM06	2.1	0.012	4.6	NA
MN15-L	2.3	0.012	5.9	1
M11plus	2.1	0.012	6.3	NA
PW6B95-D3(BJ)	5.8	0.010	6.5	NA
M11pz	2.8	0.009	7.2	2
PW6B95	6.3	0.008	7.3	NA
revM06-L	2.7	0.009	7.6	3
B97-1	2.9	0.015	7.6	NA
M06-L	3.1	0.007	9.0	4
GAM	3.9	0.019	10.4	5
B3LYP	4.5	0.017	11.3	NA
PBE	6.5	0.016	11.3	6
TPSS	4.9	0.012	11.4	7
OreLYP	4.6	0.020	11.6	8
BLYP	5.6	0.027	14.0	9

[a]The overall MUEs are calculated by eq 9 over the 27 energetic databases in Table 4 and over the two geometric databases in Table 4. The average ranks of the 16 functionals are obtained by ranking the functionals over each of the 29 databases and then averaging the 29 ranks. The PEC37 and LC18 databases of Table 1 are not considered here. [b]The rank is based on the previous column (the average rank column). [c]NA denotes not applicable.

Table 5 shows that MN15, which is a global-hybrid exchange-correlation functional, performs the best of the 16 compared functionals, with an average rank of 3.9. The next five are revM06, MN15-L, M11plus, PW6B95-D3(BJ), and M11pz, in that order. The table shows that M11pz is two ranks lower than the M11plus functional that has the same functional form but with HF exchange also present; this is not surprising since HF exchange often improves overall performance on databases that have more weakly correlated systems than strongly correlated systems.

We can also make a comparison considering only the nine nonhybrid functionals. When judged by performance on the 29 databases of Table 4, the best nonhybrid functional is MN15-L, and the second best is M11pz (see Table 5). The popular PBE local functional is ranked sixth out of nine nonhybrid functionals, and the historically important BLYP functional (the first functional to have a large impact in computational chemistry[70]) is ranked ninth. The difference between BLYP and the top-ranked functionals is a measure of the historical progress in density functional development.

Next, we broaden the evaluation of the nine nonhybrid functionals to include databases in Table 2 not used in the training of M11pz. Table 6 gives the performance of 10 functionals—the eight local functionals, M11plus, and M11pz, on a subset of the individual databases of Table 2 (all except the PEC150, TMOBG4, and SBG31 databases). Table 7 gives results for eight combined databases that we made by grouping the databases from Tables 4 and 6; the combined databases contain atomic and molecular energies (AME418/22), main-group bond energies (MGBE172), transition-metal bond energies (TMBE40), single-reference systems (SR309), multi-reference systems (MR54), barrier heights (BH192), non-covalent systems (NC579), and molecular structures (MS20). The details of which databases and systems are classified as single-reference (SR309) and multireference (MR54) are given in Tables S59 and S60 of the Supporting Information and Tables S2 and S3 of ref 18. The details of the errors on each database in each combined database are provided in the Supporting Information. The broader data is discussed in the following subsections.

3.1. Ground-State Properties. *3.1.1. Main-Group Bond Energies.* The performance of 10 functionals on the main-group bond energies database is shown for database MGBE172 in Table 7. The hybrid functional M11plus shows the best accuracy with the lowest MUE of 1.8 kcal/mol. The best nonhybrid functionals in the table are MN15-L, revM06-L, and M11pz, in that order; therefore, M11pz performed better than the remaining six tested local functionals. Figure 1 illustrates the MUEs on the databases (MGM-BE12, MGN-BE140, YBDE18, and ASNC2) that make up MGBE172. Most of the functionals have similar performance on main-group non-metal-bond energies (MGN-BE140, red line), but there are significant differences for ylide bond dissociation energies (YBDE18, gray line) and atmospheric sulfur-nitrogen cluster binding energies (ASNC2, yellow line). Even though MN15-L shows the lowest MUE among local functionals for the combined database MGBE172, it has a significantly higher MUE on ASNC2 than revM06-L and M11pz. For M11pz, the highest MUE on any of the four subsets of the combined database is 5.0 kcal/mol, which is lower than the highest MUEs of the other local functionals (which are in the range 5.5−15.7 kcal/mol). This illustrates the success of the present design strategy at keeping the errors down across-the-board.

3.1.2. Transition-Metal Bond Energies. Bond energies of several molecules containing transition metals are combined in TMBE40 in Table 7. This database combines SR-TM-BE15, MR-TM-BE13, MR-TMD-BE3, and WCCR9/18. M11pz shows the best performance on TMBE40, with an MUE of 4.5 kcal/mol and it also performs better than M11plus (5.8 kcal/mol).

Figure 2 shows individual results for each database in TMBE40. All functionals except OreLYP have their highest MUE for the multireference transition-metal dimer bond energies (MR-TMD-BE3) database. M11pz is the fourth best of the 10 functionals for MR-TMD-BE3. Most hybrid functionals do poorly on MR-TMD-BE3, as shown in Table 3 of ref 18. Compared to M11plus, M11pz significantly improves the MUE of SR-TM-BE15, MR-TM-BE13, and MR-TMD-BE3

https://doi.org/10.1021/acs.jctc.2c01315
J. Chem. Theory Comput. 2023, 19, 9102−9117

Table 6. Mean Unsigned Errors (MUEs) on 20 Databases in the Testing Set for M11plus and Nine Nonhybrid Functionals

database	M11plus	BLYP	PBE	OreLYP	GAM	TPSS	M06-L	MN15-L	revM06-L	M11pz
					MUEs in kcal/mol					
AL2X6	0.5	12.0	4.3	14.6	7.1	4.0	0.8	1.4	1.5	3.0
ASNC2	1.5	7.7	2.7	15.7	5.5	3.6	3.4	7.6	6.4	3.7
BHDIV10	1.8	5.3	8.2	4.8	4.6	6.1	3.1	2.1	2.4	3.0
BHPERI26	2.5	4.6	3.9	6.3	2.5	2.2	1.9	1.8	3.9	3.1
BHROT27	0.3	0.4	0.5	0.4	0.7	0.5	1.0	0.9	1.1	0.8
DIPCS10	4.2	7.9	4.6	6.3	7.8	3.8	8.4	10.3	9.5	6.5
HeavySB11	0.8	8.1	4.6	9.3	5.1	4.4	2.7	6.5	2.7	7.9
PX13	5.0	7.0	11.6	5.8	1.6	8.4	0.9	6.4	6.0	3.7
SIE4x4	7.2	24.7	23.4	24.2	22.9	21.5	17.9	11.0	14.2	14.2
S66x8	0.32	2.95	1.50	4.61	0.83	2.10	0.46	1.06	0.45	0.35
YBDE18	2.0	11.1	5.9	9.8	4.7	7.3	4.9	4.2	5.5	5.0
TMBH22	2.4	4.4	3.5	5.2	3.4	2.7	2.7	1.9	2.5	2.4
WCCR9/18	4.9	9.1	7.2	13.7	5.3	7.4	5.2	4.7	5.2	5.2
ALKBDE10	2.9	5.7	6.2	4.3	3.6	4.1	5.2	4.5	4.7	4.5
RSE43	0.3	3.1	3.1	3.5	3.0	2.2	2.7	1.2	2.3	1.4
WCPT18	2.5	4.1	8.6	4.2	2.8	5.5	2.1	1.8	1.9	2.4
W4-11	3.5	7.4	15.0	6.4	5.5	5.0	4.3	3.2	4.1	4.6
MOR41	3.6	13.5	7.9	18.1	11.5	7.8	5.8	3.2	5.1	8.0
					MUEs in debye					
DM79	0.29	0.30	0.29	0.31	0.26	0.26	0.25	0.27	0.27	0.27
					MUEs in Å					
TMDBL10	0.058	0.047	0.043	0.048	0.065	0.056	0.057	0.059	0.072	0.065

Table 7. Mean Unsigned Errors[a] on Eight Combined Databases for M11plus and Nine Nonhybrid Functionals

database	M11plus	BLYP	PBE	OreLYP	GAM	TPSS	M06-L	MN15-L	revM06-L	M11pz
AME418/22[b]	2.2	5.5	6.8	4.1	4.0	4.8	3.2	2.2	2.9	2.8
MGBE172[c]	1.8	4.9	4.8	4.5	3.2	3.8	2.9	2.2	2.4	2.8
TMBE40[d]	5.8	9.9	8.8	7.9	5.5	6.4	4.8	5.0	6.1	4.5
SR309[e]	1.8	5.4	5.0	4.4	4.0	4.8	3.4	2.1	3.0	3.0
MR54[f]	5.3	12.0	11.2	7.6	6.5	7.1	4.9	3.8	4.5	4.3
BH192[g]	1.8	5.6	6.6	5.0	3.6	5.5	2.8	2.0	2.5	2.7
NC579[h]	0.32	2.84	1.46	4.43	0.83	2.02	0.46	1.02	0.45	0.37
MS20[i] (Å)	0.035	0.037	0.029	0.034	0.042	0.034	0.032	0.035	0.041	0.037
average rank	2.6	9.3	8.0	7.4	6.1	7.0	4.0	2.9	4.3	3.5
final rank	1	10	9	8	6	7	4	2	5	3

[a]Errors in kcal/mol except where indicated otherwise. [b]AME418/22 is the union of SR-MGM-BE8, SR-MGN-BE107, SR-TM-BE15, MR-MGM-BE4, MR-MGN-BE17, MR-TM-BE13, IsoL6/11, IP23, EA13/03, PA8, πTC13, HTBH38/08, NHTBH38/08, NCCE23/18, CT7/04, AE17, HC7/11, 3dEE7/22, 4dAEE5, pAEE5, DC9/19, pBIsoE8, NGD21/18, MR-TMD-BE3, and SMAE3/19. [c]MBGE172 is the union of MGM-BE12 (combination of SR-MGM-BE8 and MR-MGM-BE4), MGN-BE140 (combination of SR-MGN-BE107, MR-MGN-BE17, SMAE3/19, and ABDE13), YBDE18, and ASNC2. [d]TMBE40 is combined from SR-TM-BE15, MR-TM-BE13, MR-TMD-BE3, and WCCR9/18. [e]SR309 is combined from SR-MGM-BE8, SR-MGN-BE107, SR-TM-BE15, HTBH38/18 (37 data), NHTBH38/18 (35 data), 3dEE7/22, 4dAEE5, pAEE5, pBIsoE8, IsoL6/11, πTC13, HC7/11 (4 data), EA13/03, PA8, IP23, SMAE3/19 (1 datum), DC9/19 (1 datum), and ABDE13. [f]MR54 is the combination of MR-MGM-BE4, MR-MGN-BE17, MR-TM-BE13, MR-TMD-BE3, HTBH38/18 (1 datum), NHTBH38/18 (3 data), HC7/11 (3 data), SMAE3/19 (2 data), and DC9/19 (8 data). [g]BH192 is the combination of HTBH38/08, NHTBH38/08, BHDIV10, BHPERI26, BHROT27, PX13, TMBH22, and WCPT18. [h]NC579 is the combination of NCCE23/18, CT7/04, NGD21/18, and S66x8 databases. [i]MS20 is the combination of DGL6, DGH4, and TMDBL10.

and has a similar MUE for WCCR9/18. Thus, removing HF exchange broadly improves the performance for transition-metal systems.

3.1.3. Single-Reference Systems. To address how each functional performs on specifically SR systems, we combined 18 SR training databases in SR309, as shown in Table 7. M11pz performed well with an MUE of 3.0 kcal/mol, and it is the fourth best after M11plus, MN15-L, and revM06-L. This means M11pz is the third best among nine nonhybrid functionals.

3.1.4. Multireference Systems. Previous work showed that M11plus, which has the same range-dependent percentage of HF exchange as M11, but has rung-3.5 terms added, has a lower MUE on MR53 than M11 (see Table 4 of ref 18). It also performed better than other global hybrid functionals, except MN15.[18] In this work, we added the bond energy of FeO^+ to MR-TM-BE12, which is a subset of the multireference MR53 database; therefore, MR-TM-BE12 becomes MR-TM-BE13 and MR53 becomes MR54. M11pz shows a striking result for MR54; its MUE of 4.3 kcal/mol is 1.0 kcal/mol lower than that of M11plus. The only functional in Table 7 that does better than M11pz is MN15-L with an MUE of 3.8 kcal/mol. The revM06-L and M06-L functionals perform the third and fourth best among the 10 functionals with a small difference between them. The PBE and BLYP functionals, although they do not suffer from the

https://doi.org/10.1021/acs.jctc.2c01315
J. Chem. Theory Comput. 2023, 19, 9102−9117

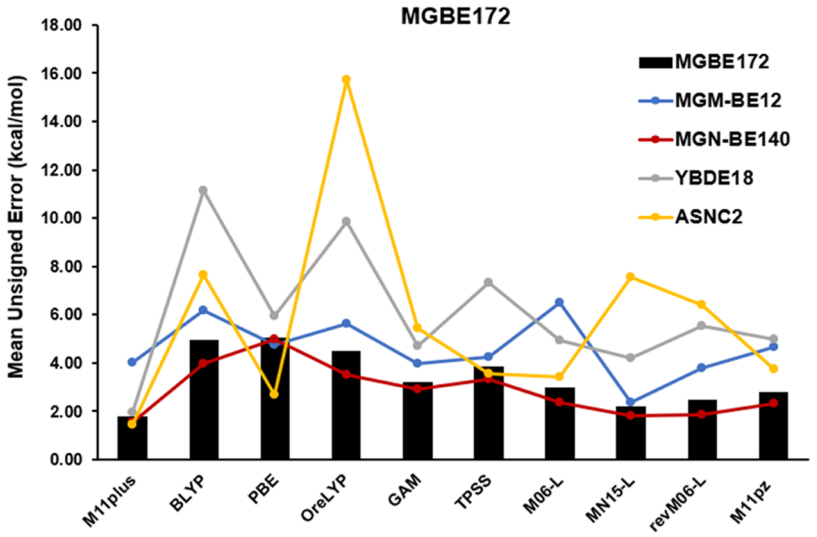

Figure 1. Mean unsigned errors on the main-group bond energies database (MGBE172) and on the individual subdatabases making up MGBE172: MGM-BE12 (the combination of SR-MGM-BE8 and MR-MGM-BE4), MGN-BE140 (the combination of SR-MGN-BE107, MR-MGN-BE17, SMAE3/19, and ABDE13), YBDE18, and ASNC2. The black bars in the figure show the overall MUE of all four databases (combined as MGBE172), which is the same MUE as shown in Table 7.

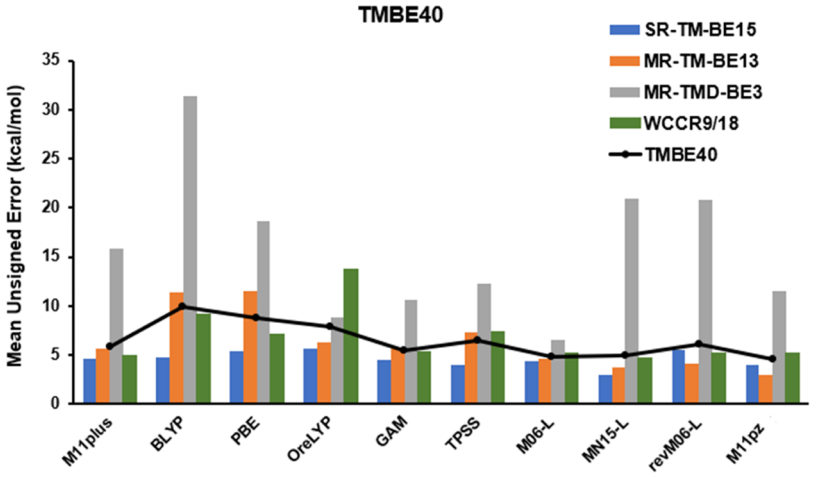

Figure 2. Mean unsigned errors on the transition-metal bond energies database, TMBE40 (black curve), and its individual subdatabases, SR-TM-BE15, MR-TM-BE13, MR-TMD-BE3, and WCCR9/18.

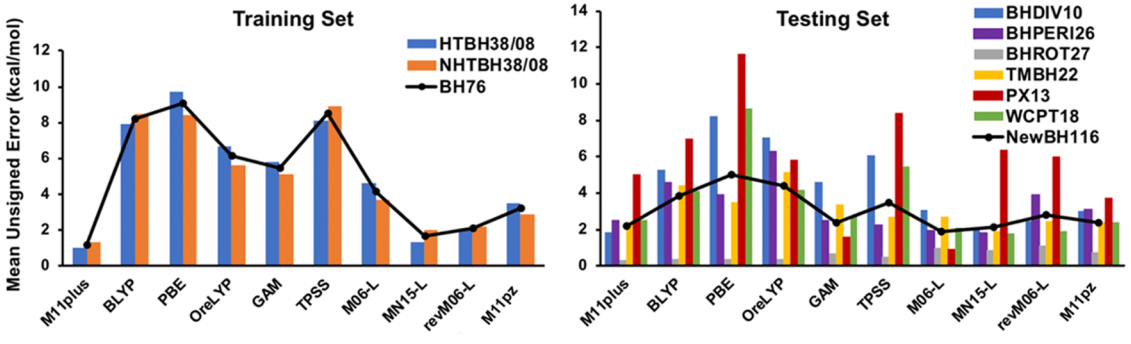

Figure 3. (Left) Mean unsigned errors on barrier heights in the training-and-testing set, BH76, and its subdatabases, HTBH38/08 and NHTBH38/08. (Right) Mean unsigned errors on barrier heights in the testing set, NewBH116, and its subdatabases, BHDIV10, BHPERI26, BHROT27, TMBH22, PX13, and WCPT18.

static correlation error of HF exchange, perform least well, and show high MUEs of 11−12 kcal/mol, which is larger than that of M11pz by 7−8 kcal/mol. The good success of M11pz for MR54 is very gratifying since one of our principal design goals was to obtain improved performance for MR systems.

3.1.5. Barrier Heights. Several databases of barrier heights including two databases from the training-and-testing set and six

https://doi.org/10.1021/acs.jctc.2c01315
J. Chem. Theory Comput. 2023, 19, 9102−9117

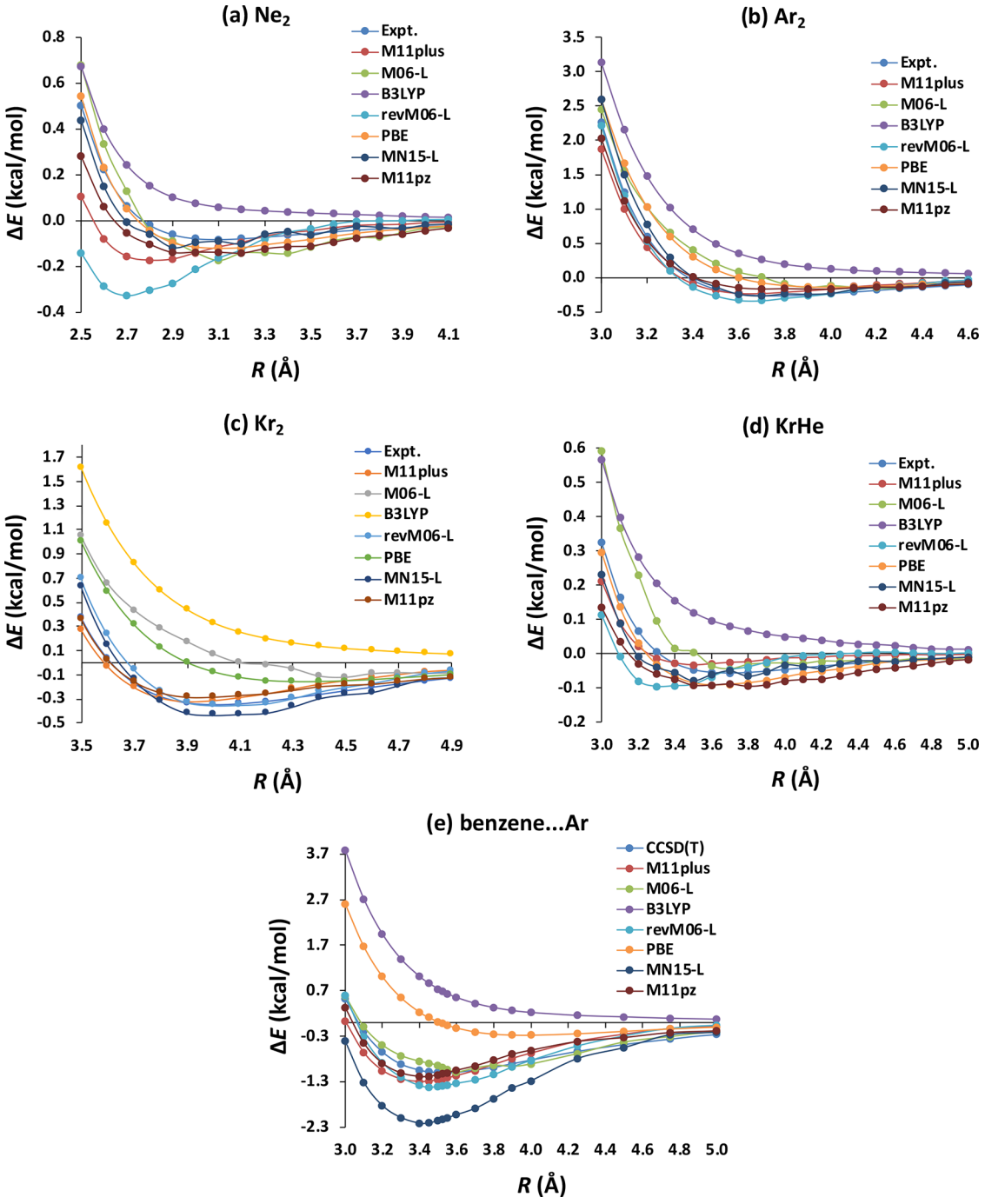

Figure 4. Potential energy curves of four inert-gas dimers (Ne_2, Ar_2, Kr_2, and KrHe) and benzene···Ar complex calculated by seven density functionals—B3LYP, M11plus, PBE, M06-L, MN15-L, revM06-L, and M11pz. The reference values are obtained using CCSD(T) and aug-cc-pVQZ basis set for the benzene···Ar complex.

databases from the testing set are combined into BH192 with 192 data. The training-and-testing databases are hydrogen-transfer barrier heights (HTBH38/08) and non-hydrogen-transfer barrier heights (NHTBH38/08). The testing-only databases are combined into a database called NewBH116, consisting of barrier heights of diverse reactions (BHDIV10), barrier heights of pericyclic reactions (BHPERI26), barrier heights for rotation around single bonds (BHROT27), transition-metal reaction barrier heights of Mo, W, Zr, and Re reactions (TMBH22), proton-exchange barriers in H_2O, NH_3, and HF clusters (PX13), and proton-transfer barriers in uncatalyzed and water-catalyzed reactions (WCPT18).

Table 7 shows that the hybrid functional M11plus has the lowest MUE of 1.8 kcal/mol followed by MN15-L (2.0 kcal/mol), revM06-L (2.5 kcal/mol), and M11pz (2.7 kcal/mol).

Figure 3 shows the performance of individual databases in BH192. The M11pz performance is in the top four out of 10 functionals for BH76 and in the top five out of 10 functionals for NewBH116. In keeping with our goal of good across-the-board performance, Figure 3 shows that M11pz does not have a

https://doi.org/10.1021/acs.jctc.2c01315
J. Chem. Theory Comput. 2023, 19, 9102−9117

particularly large error on any of the constituent databases, with the largest MUE being 3.7 kcal/mol on PX13.

3.1.6. Noncovalent Interactions. The combination of all noncovalent interactions databases produces a new database called NC579. This is the union of noncovalent complexation energies (NCCE23/18), charge transfer noncovalent complexes (CT7/04), noble gas dimer weak interactions (NGD21/18), and noncovalent interaction energies of complexes relevant to biomolecules (S66x8) databases. In Table 7, we see that 5 out of 10 compared functionals have MUEs less than 1.0 kcal/mol, with the five best functionals, in order being M11plus, M11pz, revM06-L, M06-L, and GAM. M11pz has an MUE of 0.37 kcal/mol, which is only 0.04 kcal/mol higher than M11plus.

Figure 4 shows potential energy curves obtained with seven functionals (B3LYP, M11plus, PBE, M06-L, MN15-L, revM06-L, and M11pz) for four van der Waals inert gas molecules: Ne_2, Ar_2, Kr_2, and KrHe and the van der Waals complex, benzene···Ar (PEC150 database). The results are compared to experiment (Expt.)[71] in the first four cases and to CCSD(T) calculations[33] for benzene···Ar. Some points of the PEC150 database overlap with the training data. The binding energies near the equilibrium for Ne_2, Ar_2, and Kr_2 are in the NGD21/18 training database, and points on the repulsive walls of Ne_2, Ar_2, Kr_2, KrHe, and benzene···Ar are in the PEC37 training database. However, the long-range tail and some other parts of the potential energy curves are not included, and here we test the performance of seven functionals on the whole curve. As stated earlier, we also added benzene···Ar complex as a new system in the training-and-testing and testing databases. Figure 4 shows that B3LYP has a positive interaction energy (ΔE) at all intermonomer distances for all five systems, while the other functionals show some binding, although PBE and M06-L yield notably too shallow minima compared with other functionals for Ar_2 and Kr_2. The M11pz functional (in dark brown) performs exceptionally well on the repulsive parts of the potential (which are at distances less than the equilibrium distance), although there is still room for improvement for Ne_2 and KrHe. The M11pz functional improves the accuracy compared to M11plus at several separations for all systems except KrHe. The M11pz shows smoother potential energy curves than M06-L, MN15-L, and revM06-L.

3.1.7. Molecular Structures. The molecular-geometry databases are combined into the MS20 database; MS20 includes diatomic bond lengths for diatomic molecules with light atoms (DGL6), diatomic bond lengths for diatoms with one or more heavy atoms (DGH4), and transition-metal dimer bond lengths (TMDBL10). Table 7 gives the MUEs on this database; the three functionals with the smallest MUE in calculating the bond lengths are PBE, M06-L, and TPSS, in that order. The M11pz functional has MUE 0.008 Å higher than the best and has a similar performance to M11plus, even though it has less ingredients.

3.1.8. Self-Interaction Errors. Self-interaction error is one of the major sources of error in Kohn−Sham DFT.[72−75] It is well known[76] that HF exchange cancels the interaction of an electron with itself, and therefore self-interaction error is ameliorated by adding some HF exchange into the functional form. We investigate this error by studying the SIE4x4 database consisting of four doublet cation complexes (H_2^+, He_2^+, $(NH_3)_2^+$, and $(H_2O)_2^+$). The MUEs of 10 functionals on this database are given in Table 6. The M11plus functional is the only one of these functionals that has some fraction of HF exchange, and it provides the best results with the lowest MUE of 7.2 kcal/mol. The best local functional for self-interaction error is MN15-L with an MUE of 11.0 kcal/mol. The next best functionals are M11pz and revM06-L. By referring to Table 13 of ref 26, one can see that M11pz with its MUE of 14.2 kcal/mol performs better than B3LYP, which is a hybrid functional with an MUE of 17.6 kcal/mol. However, M11pz is still not as accurate for this test as several long-range-corrected functionals, such as CAM-B3LYP, M11, and revM11, whose results are in Table 13 of ref 26. This is consistent with the observation made above that nonhybrid functionals tend to provide higher self-interaction error than hybrid functionals with some percentage of HF exchange.

3.1.9. Dipole Moments. The dipole moment is the first moment of a charge distribution and is therefore very relevant to the question of whether a functional gives a good density. We test this with the DM79 database of dipole moments of 79 molecules. For this test, we do single-point calculations at the same geometries as used in making the database. The errors calculated for this database are shown in Table 6. All functionals tested have similar MUEs, which fall in the range of 0.25−0.31 debye.

3.2. Atomic and Molecular Energies (AME418/22). This database is a superset of 25 databases (Table S56) from the training-and-testing set of MDB, combining most of ground-state-energy databases and all three excitation-energy databases calculated by the ΔSCF method, but excluding DGL6, DGH4, ABDE13, S6x6, LC18, and PEC37. The M11plus and MN15-L functionals provide the best MUEs of 2.2 kcal/mol on AME418/22 (see Table 7). The new M11pz is unable to improve on the performance of MN15-L, but it gets a similar MUE (2.8 kcal/mol) as revM06-L, and these functionals are next best behind MN15-L, among all of the nonhybrid functionals tested.

3.3. Excited-State Properties. The training-and-testing set for functional optimization includes three excitation-energy databases, 3dEE7/22, 4dAEE5, and pAEE5, in which vertical excitation energies are calculated by using the ΔSCF method. The MUEs for the three databases with various functionals are shown in Table 4, and the overall MUE of these three databases combined as EE17 is shown in Figure 5. The lowest MUE of this database is obtained with the MN15-L functional. The M11pz is the second best, giving a slight improvement over M11plus.

3.4. Performance of Functionals Based on Maximum Absolute Error. We have so far discussed the performance of functionals based on their MUEs; next, we present their performance based on maximum absolute errors. The ranks of

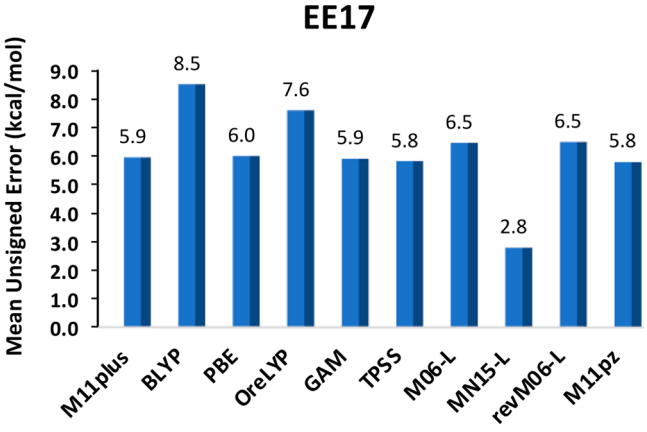

Figure 5. Mean unsigned errors on training-and-testing excitation-energies database, EE17 (combining 3dEE7/22, 4dAEE5, and pAEE5).

https://doi.org/10.1021/acs.jctc.2c01315
J. Chem. Theory Comput. 2023, 19, 9102−9117

10 functionals (M11plus + nine nonhybrid functionals) based on their maximum absolute errors on 43 databases from MDB are shown in Table 8 (details of what databases are included can be found in Table S65). The MUEs of these 43 databases are in Tables 4 and 6.

Table 8. Average Rank and Final Rank of 10 Functionals based on their Maximum Absolute Errors on 43 Databases[a] from MDB

functional	average rank	final rank
M11plus	3.3	1
MN15-L	4.0	2
M11pz	4.3	3
M06-L	4.9	4
revM06-L	5.2	5
TPSS	6.0	6
GAM	6.0	7
PBE	6.5	8
OreLYP	7.0	9
BLYP	7.9	10

[a]The 43 databases are listed in Table S65. Their MUEs are presented in Tables 4 and 6.

Based on average rank using maximum absolute error, the M11pz functional is in the third place among the 10 functionals and second best among the nonhybrid functionals after MN15-L. It is very encouraging that M11pz shows one of the best average ranks among the nine tested nonhybrid functionals both in the rankings based on MUE and the rankings based on maximum absolute error.

3.5. Solid-State Databases. We consider three solid-state databases: lattice constants of 17 solids (LC18), band gaps of 31 semiconductors (SBG31), and band gaps of four transition-metal oxides (TMOBG4). LC18 was part of the training-and-testing set, and the other two are used only for testing. Table 9 and Figure 6 show MUEs calculated for each database by M11pz and eight local functionals. For the calculation of lattice constants, revM06-L has the lowest MUE, and M11pz is fifth out of nine functionals. However, M11pz performs second best for semiconductor band gaps and second best for transition-metal oxide band gaps. We averaged the rank of each functional on these three databases and found that revM06-L is the best, and M11pz shares the second rank with MN15-L.

We also present the ranks of nine nonhybrid functionals based on maximum absolute errors on these three solid-state databases in Table S66. The best five functionals in Table S66 are M11pz, revM06-L, MN15-L, TPSS, and OreLYP, in that order.

3.6. Other Databases. We performed calculations on five other databases that are not in MDB. The MUE of each database is shown in Table 6 and Figure 7.

First, we discuss results on four databases from GMTKN55,[43] namely, ALKBDE10, RSE43, WCPT18, and W4-11. Figure 7 shows that M11plus and MN15-L perform the best on average. The M06-L, revM06-L, and M11pz functionals also generally provide lower MUEs than BLYP, PBE, OreLYP, GAM, and TPSS. We present the MUEs and ranks of M11pz, M11plus, and eight local functionals on these four databases from GMTKN55 in Table 10.

We also compared the performance of M11pz for these four databases from GMTKN55 with a group of 29 hybrid functionals that do not have molecular mechanics terms. In the GMTKN55 paper;[43] these 29 functionals (which are the same ones discussed in the M11plus paper) were selected mainly based on good performance in previous tests and/or high popularity. We compared the performance of M11pz to these functionals for RSE43, ALKBDE10, WCPT18, and W4-11, and the comparison is shown in Table S67. The average MUEs calculated by the 30 functionals are given in Table S67 for RSE43, ALKBDE10, WCPT18, and W4-11 and are 1.58, 4.96, 2.45, and 4.88 kcal/mol, respectively. The MUEs from M11pz are 1.43, 4.51, 2.43, and 4.58 kcal/mol, in the same order, which indicates that M11pz performs better than the average of these hybrid functionals for all four databases (which were not used for training), which is very encouraging.

We also consider a database of closed-shell metal-organic reactions, namely, MOR41, which is not in MDB. For MOR41, the MN15-L and M11plus functionals performed the first and second best, respectively, with all the MUEs shown in Table 6. M11pz ranks 7th out of 10 functionals. Although M11pz did not perform better for this database than MN15-L, M11plus, revM06-L, or M06-L, it performs approximately the same as PBE and much better than BLYP, OreLYP, or GAM.

4. CONCLUSIONS

We have presented a new meta nonlocal functional M11pz with zero HF exchange; it is built on the previously developed functional M11plus that has rung-3.5 ingredients. The main set of results presented in this work (summarized in Table 7) show that, among the tested nonhybrid functionals, M11pz has the second best accuracy on average when errors are calculated from the combined databases with a variety of atomic and molecular properties. Additionally, on average M11pz also performs the

Table 9. Mean Unsigned Errors (MUEs) and Ranks Based on MUEs of LC18, SBG31, and TMOBG4 Databases Calculated Using M11pz and Eight Other Functionals with Zero Hartree−Fock Exchange

	LC18		SBG31		TMOBG4			
functional	MUE (Å)	rank	MUE (eV)	rank	MUE (eV)	rank	average rank	final rank
BLYP	0.111	8	0.96	8	2.85	7	7.7	9
PBE	0.066	4	1.01	9	2.90	9	7.3	7
OreLYP	0.112	9	0.77	5	2.86	8	7.3	7
GAM	0.089	7	0.78	6	2.77	6	6.3	6
TPSS	0.053	3	0.88	7	2.64	5	5.0	5
M06-L	0.079	6	0.64	3	2.36	3	4.0	4
MN15-L	0.051	2	0.76	4	2.36	3	3.0	2
revM06-L	0.040	1	0.48	1	1.53	1	1.0	1
M11pz	0.074	5	0.51	2	1.90	2	3.0	2

https://doi.org/10.1021/acs.jctc.2c01315
J. Chem. Theory Comput. 2023, 19, 9102−9117

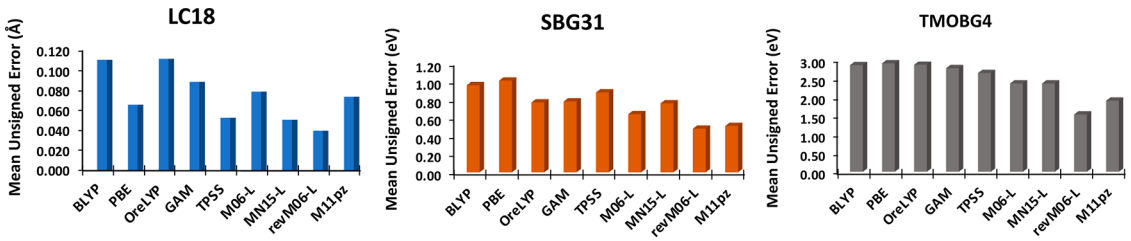

Figure 6. Mean unsigned errors on lattice constants database, LC18, on semiconductor band gaps database, SBG31, and on transition-metal oxide band gaps database, TMOBG4.

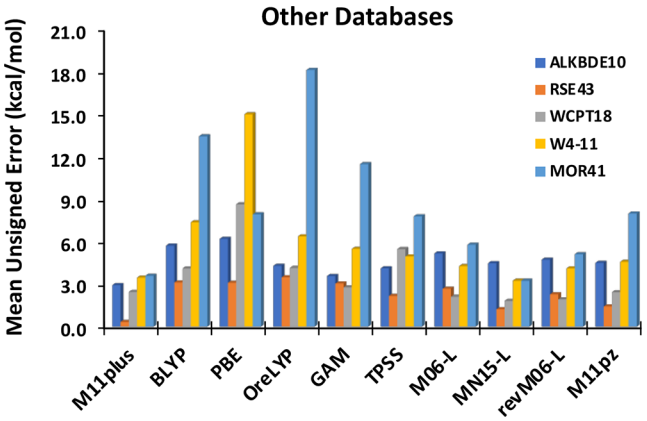

Figure 7. Mean unsigned errors on other databases that are not in MDB, which include ALKBDE10, RSE43, WCPT18, W4-11, and MOR41.

second best on the solid-state databases shown in Table 9. Its performance is as good as or even better than our previously developed local functionals MN15-L, revM06-L, and M06-L. The comparison to MN15-L is more equivocal; if we form a judgment based on MUEs, MN15-L has better performance than M11pz for several combined databases including MR54, and the average rank of M11pz is similar to that of MN15-L.

The M11pz functional differs from local functionals by the rung-3.5 terms that account for static correlation, which is important for strongly correlated systems. This helps M11pz to perform better than local functionals for calculations on multireference systems, transition-metal systems, solid-state systems, and noncovalent systems.

■ ASSOCIATED CONTENT

Supporting Information

The Supporting Information is available free of charge at https://pubs.acs.org/doi/10.1021/acs.jctc.2c01315.

Reference values, calculated values, mean unsigned errors, maximum absolute errors, ranks for various databases, and absolute energies with the newly optimized functional, M11pz (PDF)

■ AUTHOR INFORMATION

Corresponding Authors

Pragya Verma − *Department of Chemistry, Chemical Theory Center, and Minnesota Supercomputing Institute, University of Minnesota, Minneapolis, Minnesota 55455-0431, United States;* orcid.org/0000-0002-5722-0894; Email: verma045@umn.edu

Donald G. Truhlar − *Department of Chemistry, Chemical Theory Center, and Minnesota Supercomputing Institute, University of Minnesota, Minneapolis, Minnesota 55455-0431, United States;* orcid.org/0000-0002-7742-7294; Email: truhlar@umn.edu

Authors

Siriluk Kanchanakungwankul − *Department of Chemistry, Chemical Theory Center, and Minnesota Supercomputing Institute, University of Minnesota, Minneapolis, Minnesota 55455-0431, United States;* orcid.org/0000-0003-4906-020X

Benjamin G. Janesko − *Department of Chemistry and Biochemistry, Texas Christian University, Fort Worth, Texas 76110, United States;* orcid.org/0000-0002-2572-5273

Giovanni Scalmani − *Gaussian, Inc., Wallingford, Connecticut 06492, United States;* orcid.org/0000-0002-4597-7195

Table 10. Ranks of 10 Functionals Based on Mean Unsigned Errors (MUEs) on Four Databases from GMTKN55

	ALKBDE10		RSE43		WCPT18		W4-11			
functional	MUE	rank	MUE	rank	MUE	rank	MUE	rank	average rank	final rank[a]
M11plus	2.9	1	0.3	1	2.5	5	3.5	2	2.3	1
MN15-L	4.5	5	1.2	2	1.8	1	3.2	1	2.3	1
revM06-L	4.7	7	2.3	5	1.9	2	4.1	3	4.3	3
M11pz	4.5	6	1.4	3	2.4	4	4.6	5	4.5	4
M06-L	5.2	8	2.7	6	2.1	3	4.3	4	5.3	5
GAM	3.6	2	3.0	7	2.8	6	5.5	7	5.5	6
TPSS	4.1	3	2.2	4	5.5	9	5.0	6	5.5	6
OreLYP	4.3	4	3.5	10	4.2	8	6.4	8	7.5	8
BLYP	5.7	9	3.1	9	4.1	7	7.4	9	8.5	9
PBE	6.2	10	3.1	8	8.6	10	15.0	10	9.5	10

[a]Final rank is based on the previous column and hence refers only to these four databases.

https://doi.org/10.1021/acs.jctc.2c01315
J. Chem. Theory Comput. 2023, 19, 9102−9117

Michael J. Frisch − *Gaussian, Inc., Wallingford, Connecticut 06492, United States*

Complete contact information is available at: https://pubs.acs.org/10.1021/acs.jctc.2c01315

Author Contributions

‖S.K. and P.V. are co-first authors.

Notes

The authors declare no competing financial interest.

■ ACKNOWLEDGMENTS

This work was supported by the National Science Foundation under grant CHE-2054723.

■ REFERENCES

(1) Kohn, W.; Sham, L. J. Self-Consistent Equations Including Exchange and Correlation Effects. *Phys. Rev.* **1965**, *140*, A1133−A1138.
(2) Kohn, W. Nobel Lecture: Electronic Structure of Matter-Wave Functions and Density Functionals. *Rev. Mod. Phys.* **1999**, *71*, 1253−1266.
(3) Verma, P.; Truhlar, D. G. Status and Challenges of Density Functional Theory. *Trends Chem.* **2020**, *2*, 302−318.
(4) Polo, V.; Kraka, E.; Cremer, D. Electron Correlation and the Self-Interaction Error of Density Functional Theory. *Mol. Phys.* **2002**, *100*, 1771−1790.
(5) Gräfenstein, J.; Cremer, D. The Self-Interaction Error and the Description of Non-Dynamic Electron Correlation in Density Functional Theory. *Theor. Chem. Acc.* **2009**, *123*, 171−182.
(6) Scuseria, G. E.; Staroverov, V. N. Progress in the Development of Exchange-Correlation Functionals. In *Theory and Applications of Computational Chemistry: The First 40 Years*; Dykstra, C. E.; Frenking, G.; Kim, K. S.; Scuseria, G. E., Eds.; Elsevier: Amsterdam, 2006; pp 669−724.
(7) Peverati, R.; Truhlar, D. G. Quest for a Universal Density Functional: The Accuracy of Density Functionals Across a Broad Spectrum of Databases in Chemistry and Physics. *Philos. Trans. R. Soc., A* **2014**, *372*, No. 20120476.
(8) Becke, A. D. A New Mixing of Hartree−Fock and Local Density-Functional Theories. *J. Chem. Phys.* **1993**, *98*, 1372−1377.
(9) Toulouse, J.; Colonna, F.; Savin, A. Long-Range−Short-Range Separation of the Electron-Electron Interaction in Density-Functional Theory. *Phys. Rev. A: At., Mol., Opt. Phys.* **2004**, *70*, No. 062505.
(10) Jaramillo, J.; Scuseria, G. E.; Ernzerhof, M. Local Hybrid Functionals. *J. Chem. Phys.* **2003**, *118*, 1068−1073.
(11) Maier, T. M.; Arbuznikov, A. V.; Kaupp, M. Local Hybrid Functionals: Theory, Implementation, and Performance of an Emerging New Tool in Quantum Chemistry and Beyond. *Wiley Interdiscip. Rev.: Comput. Mol. Sci.* **2019**, *9*, No. e1378.
(12) Baker, J.; Muir, M.; Andzelm, J.; Scheiner, A. Hybrid Hartree−Fock Density-Functional Theory Functionals: The Adiabatic Connection Method. In *Chemical Applications of Density-Functional Theory*; Laird, B. B.; Ross, R. B.; Ziegler, T., Eds.; ACS Symposium Series 629; American Chemical Society: Washington, D.C., 1996; pp 342−367.
(13) Vydrov, O. A.; Scuseria, G. E. Assessment of a Long-Range Corrected Hybrid Functional. *J. Chem. Phys.* **2006**, *125*, No. 234109.
(14) Brütting, M.; Bahmann, H.; Kümmel, S. Hybrid Functionals with Local Range Separation: Accurate Atomization Energies and Reaction Barrier Heights. *J. Chem. Phys.* **2022**, *156*, No. 104109.
(15) Schultz, N. E.; Zhao, Y.; Truhlar, D. G. Density Functionals for Inorganometallic and Organometallic Chemistry. *J. Phys. Chem. A* **2005**, *109*, 11127−11143.
(16) Schultz, N. E.; Zhao, Y.; Truhlar, D. G. Databases for Transition Element Bonding: Metal−Metal Bond Energies and Bond Lengths and Their Use To Test Hybrid, Hybrid Meta, and Meta Density Functionals and Generalized Gradient Approximations. *J. Phys. Chem. A* **2005**, *109*, 4388−4403.
(17) Janesko, B. G. Unification of Perdew-Zunger Self-Interaction Correction, DFT+U, and Rung 3.5 Density Functionals. *J. Chem. Phys.* **2022**, *157*, No. 151101.
(18) Verma, P.; Janesko, B. G.; Wang, Y.; He, X.; Scalmani, G.; Frisch, M. J.; Truhlar, D. G. M11plus: A Range-Separated Hybrid Meta Functional with Both Local and Rung-3.5 Correlation Terms and High Across-the-Board Accuracy for Chemical Applications. *J. Chem. Theory Comput.* **2019**, *15*, 4804−4815.
(19) Peverati, R.; Truhlar, D. G. Improving the Accuracy of Hybrid Meta-GGA Density Functionals by Range Separation. *J. Phys. Chem. Lett.* **2011**, *2*, 2810−2817.
(20) Becke, A. D. Real-Space Post-Hartree-Fock Correlation Models. *J. Chem. Phys.* **2005**, *122*, No. 064101.
(21) Paier, J.; Marsman, M.; Hummer, K.; Kresse, G.; Gerber, I. C.; Ángyán, J. G. Screened Hybrid Density Functionals Applied to Solids. *J. Chem. Phys.* **2006**, *124*, No. 154709.
(22) Hasnip, P. J.; Refson, K.; Probert, M. I. J.; Yates, J. R.; Clark, S. J.; Pickard, C. J. Density Functional Theory in the Solid State. *Philos. Trans. R. Soc., A* **2014**, *372*, No. 20130270.
(23) Ashcroft, N. W.; Mermin, N. D. *Solid State Physics*; Saunders College: Philadelphia, 1976; pp 334−350.
(24) Marder, M. P. *Condensed Matter Physics*; Wiley: New York, 2000; pp 212−213, 462−464.
(25) Yu, H. S.; Li, S. L.; Truhlar, D. G. Perspective: Kohn-Sham Density Functional Theory Descending a Staircase. *J. Chem. Phys.* **2016**, *145*, No. 130901.
(26) Verma, P.; Wang, Y.; Ghosh, S.; He, X.; Truhlar, D. G. Revised M11 Exchange-Correlation Functional for Electronic Excitation Energies and Ground-State Properties. *J. Phys. Chem. A* **2019**, *123*, 2966−2990.
(27) Verma, P.; Truhlar, D. G. *Geometries for Minnesota Database 2019*; University of Minnesota, 2019. http://hdl.handle.net/11299/208752 (retrieved from the Data Repository for the University of Minnesota).
(28) Garza, A. J.; Jiménez-Hoyos, C. A.; Scuseria, G. E. Capturing Static and Dynamic Correlations by a Combination of Projected Hartree-Fock and Density Functional Theories. *J. Chem. Phys.* **2013**, *138*, No. 134102.
(29) Gao, J.; Grofe, A.; Ren, H.; Bao, P. Beyond Kohn-Sham Approximation: Hybrid Multistate Wave Function and Density Functional Theory. *J. Phys. Chem. Lett.* **2016**, *7*, 5143−5149.
(30) Zheng, P.; Gan, Z.; Zhou, C.; Su, P.; Wu, W. λ-DFVB(U): A Hybrid Density Functional Valence Bond Method Based on Unpaired Electron Density. *J. Chem. Phys.* **2022**, *156*, No. 204103.
(31) Wang, Y.; Verma, P.; Zhang, L.; Li, Y.; Liu, Z.; Truhlar, D. G.; He, X. M06-SX Screened-Exchange Density Functional for Chemistry and Solid-State Physics. *Proc. Natl. Acad. Sci. U.S.A.* **2020**, *117*, 2294−2301.
(32) Wang, Y.; Jin, X. S.; Yu, H. S.; Truhlar, D. G.; He, X. Revised M06-L Functional for Improved Accuracy on Chemical Reaction Barrier Heights, Noncovalent Interactions, and Solid-State Physics. *Proc. Natl. Acad. Sci. U.S.A.* **2017**, *114*, 8487−8492.
(33) Crittenden, D. L. A Systematic CCSD(T) Study of Long-Range and Noncovalent Interactions Between Benzene and a Series of First- and Second-Row Hydrides and Rare Gas Atoms. *J. Phys. Chem. A* **2009**, *113*, 1663−1669.
(34) Raghavachari, K.; Trucks, G. W.; Pople, J. A.; Head-Gordon, M. A Fifth-Order Perturbation Comparison of Electron Correlation Theories. *Chem. Phys. Lett.* **1989**, *157*, 479−483.
(35) Dunning, T. H. Gaussian Basis Sets for Use in Correlated Molecular Calculations. I. The Atoms Boron Through Neon and Hydrogen. *J. Chem. Phys.* **1989**, *90*, 1007−1023.
(36) Kendall, R. A.; Dunning, T. H.; Harrison, R. J. Electron Affinities of the First-Row Atoms Revisited. Systematic Basis Sets and Wave Functions. *J. Chem. Phys.* **1992**, *96*, 6796−6806.
(37) Woon, D. E.; Dunning, T. H. Gaussian Basis Sets for Use in Correlated Molecular Calculations. III. The Atoms Aluminum Through Argon. *J. Chem. Phys.* **1993**, *98*, 1358−1371.
(38) Balabanov, N. B.; Peterson, K. A. Systematically Convergent Basis Sets for Transition Metals. I. All-Electron Correlation Consistent

Basis Sets for the 3d Elements Sc−Zn. *J. Chem. Phys.* **2005**, *123*, No. 064107.
(39) Altun, A.; Breidung, J.; Neese, F.; Thiel, W. Correlated Ab Initio and Density Functional Studies on H_2 Activation by FeO^+. *J. Chem. Theory Comput.* **2014**, *10*, 3807−3820.
(40) Aguirre, F.; Husband, J.; Thompson, C. J.; Stringer, K. L.; Metz, R. B. The Low-Lying Electronic States of FeO^+: Rotational Analysis of the Resonance Enhanced Photodissociation Spectra of the $^6\Pi_{7/2} \leftarrow X\ ^6\Sigma^+$ System. *J. Chem. Phys.* **2003**, *119*, 10194−10201.
(41) Metz, R. B.; Nicolas, C.; Ahmed, M.; Leone, S. R. Direct Determination of the Ionization Energies of FeO and CuO with VUV Radiation. *J. Chem. Phys.* **2005**, *123*, No. 114313.
(42) Husband, J.; Aguirre, F.; Ferguson, P.; Metz, R. B. Vibrationally Resolved Photofragment Spectroscopy of FeO^+. *J. Chem. Phys.* **1999**, *111*, 1433−1437.
(43) Goerigk, L.; Hansen, A.; Bauer, C.; Ehrlich, S.; Najibi, A.; Grimme, S. A Look at the Density Functional Theory Zoo with the Advanced GMTKN55 Database for General Main Group Thermochemistry, Kinetics and Noncovalent Interactions. *Phys. Chem. Chem. Phys.* **2017**, *19*, 32184−32215.
(44) Dohm, S.; Hansen, A.; Steinmetz, M.; Grimme, S.; Checinski, M. P. Comprehensive Thermochemical Benchmark Set of Realistic Closed-Shell Metal Organic Reactions. *J. Chem. Theory Comput.* **2018**, *14*, 2596−2608.
(45) Verma, P.; Truhlar, D. G. Does DFT+U Mimic Hybrid Density Functionals? *Theor. Chem. Acc.* **2016**, *135*, No. 182.
(46) Weymuth, T.; Couzijn, E. P. A.; Chen, P.; Reiher, M. New Benchmark Set of Transition-Metal Coordination Reactions for the Assessment of Density Functionals. *J. Chem. Theory Comput.* **2014**, *10*, 3092−3103.
(47) Peintinger, M. F.; Oliveira, D. V.; Bredow, T. Consistent Gaussian Basis Sets of Triple-Zeta Valence with Polarization Quality for Solid-State Calculations. *J. Comput. Chem.* **2013**, *34*, 451−459.
(48) Verma, P.; Truhlar, D. G. HLE16: A Local Kohn−Sham Gradient Approximation with Good Performance for Semiconductor Band Gaps and Molecular Excitation Energies. *J. Phys. Chem. Lett.* **2017**, *8*, 380−387.
(49) Peverati, R.; Truhlar, D. G. Performance of the M11-L Density Functional for Bandgaps and Lattice Constants of Unary and Binary Semiconductors. *J. Chem. Phys.* **2012**, *136*, No. 134704.
(50) Becke, A. D. Density-Functional Exchange-Energy Approximation with Correct Asymptotic Behavior. *Phys. Rev. A* **1988**, *38*, 3098−3100.
(51) Lee, C.; Yang, W.; Parr, R. G. Development of the Colle-Salvetti Correlation-Energy Formula into a Functional of the Electron Density. *Phys. Rev. B: Condens. Matter Mater. Phys.* **1988**, *37*, 785−789.
(52) Perdew, J. P.; Burke, K.; Ernzerhof, M. Generalized Gradient Approximation Made Simple. *Phys. Rev. Lett.* **1996**, *77*, 3865−3868.
(53) Handy, N. C.; Cohen, A. J. Left-Right Correlation Energy. *Mol. Phys.* **2001**, *99*, 403−412.
(54) Thakkar, A. J.; McCarthy, S. P. Toward Improved Density Functionals for the Correlation Energy. *J. Chem. Phys.* **2009**, *131*, No. 134109.
(55) Yu, H. S.; Zhang, W.; Verma, P.; He, X.; Truhlar, D. G. Nonseparable Exchange−Correlation Functional for Molecules, Including Homogeneous Catalysis Involving Transition Metals. *Phys. Chem. Chem. Phys.* **2015**, *17*, 12146−12160.
(56) Tao, J.; Perdew, J. P.; Staroverov, V. N.; Scuseria, G. E. Climbing the Density Functional Ladder: Nonempirical Meta-Generalized Gradient Approximation Designed for Molecules and Solids. *Phys. Rev. Lett.* **2003**, *91*, No. 146401.
(57) Zhao, Y.; Truhlar, D. G. A New Local Density Functional for Main-Group Thermochemistry, Transition Metal Bonding, Thermochemical Kinetics, and Noncovalent Interactions. *J. Chem. Phys.* **2006**, *125*, No. 194101.
(58) Yu, H. S.; He, X.; Truhlar, D. G. MN15-L: A New Local Exchange-Correlation Functional for Kohn−Sham Density Functional Theory with Broad Accuracy for Atoms, Molecules, and Solids. *J. Chem. Theory Comput.* **2016**, *12*, 1280−1293.
(59) Becke, A. D. Density-Functional Thermochemistry. III. The Role of Exact Exchange. *J. Chem. Phys.* **1993**, *98*, 5648−5652.
(60) Stephens, P. J.; Devlin, F. J.; Chabalowski, C. F.; Frisch, M. J. Ab Initio Calculation of Vibrational Absorption and Circular Dichroism Spectra Using Density Functional Force Fields. *J. Phys. Chem. A* **1994**, *98*, 11623−11627.
(61) Hamprecht, F. A.; Cohen, A. J.; Tozer, D. J.; Handy, N. C. Development and Assessment of New Exchange-Correlation Functionals. *J. Chem. Phys.* **1998**, *109*, 6264−6271.
(62) Zhao, Y.; Truhlar, D. G. Design of Density Functionals That Are Broadly Accurate for Thermochemistry, Thermochemical Kinetics, and Nonbonded Interactions. *J. Phys. Chem. A* **2005**, *109*, 5656−5667.
(63) Grimme, S.; Ehrlich, S.; Goerigk, L. Effect of the Damping Function in Dispersion Corrected Density Functional Theory. *J. Comput. Chem.* **2011**, *32*, 1456−1465.
(64) Yu, H. S.; He, X.; Li, S. L.; Truhlar, D. G. MN15: A Kohn−Sham Global-Hybrid Exchange−Correlation Density Functional with Broad Accuracy for Multi-Reference and Single-Reference Systems and Noncovalent Interactions. *Chem. Sci.* **2016**, *7*, 5032−5051.
(65) Wang, Y.; Verma, P.; Jin, X. S.; Truhlar, D. G.; He, X. Revised M06 Density Functional for Main-Group and Transition-Metal Chemistry. *Proc. Natl. Acad. Sci. U.S.A.* **2018**, *115*, 10257−10262.
(66) Frisch, M. J.; Trucks, G. W.; Schlegel, H. B.; Scuseria, G. E.; Robb, M. A.; Cheeseman, J. R.; Scalmani, G.; Barone, V.; Petersson, G. A.; Nakatsuji, H.; Li, X.; Marenich, A. V.; Caricato, M.; Bloino, J.; Janesko, B. G.; Zheng, J.; Gomperts, R.; Mennucci, B.; Hratchian, H. P.; Ortiz, J. V.; Izmaylov, A. F.; Sonnenberg, J. L.; Williams-Young, D.; Ding, F.; Lipparini, F.; Egidi, F.; Goings, J.; Peng, B.; Petrone, A.; Henderson, T.; Ranasinghe, D.; Zakrzewski, V. G.; Gao, J.; Rega, N.; Zheng, G.; Liang, W.; Hada, M.; Ehara, M.; Toyota, K.; Fukuda, R.; Hasegawa, J.; Ishida, M.; Nakajima, T.; Honda, Y.; Kitao, O.; Nakai, H.; Vreven, T.; Throssell, K.; Montgomery, J. A., Jr.; Peralta, J. E.; Ogliaro, F.; Bearpark, M. J.; Heyd, J. J.; Brothers, E. N.; Kudin, K. N.; Staroverov, V. N.; Keith, T. A.; Kobayashi, R.; Normand, J.; Raghavachari, K.; Rendell, A. P.; Burant, J. C.; Iyengar, S. S.; Tomasi, J.; Cossi, M.; Millam, J. M.; Klene, M.; Adamo, C.; Cammi, R.; Ochterski, J. W.; Martin, R. L.; Morokuma, K.; Farkas, O.; Foresman, J. B.; Fox, D. J. *Gaussian Development*, version J.16; Gaussian, Inc.: Wallingford, CT, 2020.
(67) Frisch, M. J.; Trucks, G. W.; Schlegel, H. B.; Scuseria, G. E.; Robb, M. A.; Cheeseman, J. R.; Scalmani, G.; Barone, V.; Petersson, G. A.; Nakatsuji, H.; Li, X.; Caricato, M.; Marenich, A. V.; Bloino, J.; Janesko, B. G.; Gomperts, R.; Mennucci, B.; Hratchian, H. P.; Ortiz, J. V.; Izmaylov, A. F.; Sonnenberg, J. L.; Williams-Young, D.; Ding, F.; Lipparini, F.; Egidi, F.; Goings, J.; Peng, B.; Petrone, A.; Henderson, T.; Ranasinghe, D.; Zakrzewski, V. G.; Gao, J.; Rega, N.; Zheng, G.; Liang, W.; Hada, M.; Ehara, M.; Toyota, K.; Fukuda, R.; Hasegawa, J.; Ishida, M.; Nakajima, T.; Honda, Y.; Kitao, O.; Nakai, H.; Vreven, T.; Throssell, K.; Montgomery, J. A., Jr.; Peralta, J. E.; Ogliaro, F.; Bearpark, M. J.; Heyd, J. J.; Brothers, E. N.; Kudin, K. N.; Staroverov, V. N.; Keith, T. A.; Kobayashi, R.; Normand, J.; Raghavachari, K.; Rendell, A. P.; Burant, J. C.; Iyengar, S. S.; Tomasi, J.; Cossi, M.; Millam, J. M.; Klene, M.; Adamo, C.; Cammi, R.; Ochterski, J. W.; Martin, R. L.; Morokuma, K.; Farkas, O.; Foresman, J. B.; Fox, D. J. *Gaussian Development*, version I.14+; Gaussian, Inc.: Wallingford, CT, 2018.
(68) Frisch, M. J.; Trucks, G. W.; Schlegel, H. B.; Scuseria, G. E.; Robb, M. A.; Cheeseman, J. R.; Scalmani, G.; Barone, V.; Petersson, G. A.; Nakatsuji, H.; Li, X.; Caricato, M.; Marenich, A. V.; Bloino, J.; Janesko, B. G.; Gomperts, R.; Mennucci, B.; Hratchian, H. P.; Ortiz, J. V.; Izmaylov, A. F.; Sonnenberg, J. L.; Williams-Young, D.; Ding, F.; Lipparini, F.; Egidi, F.; Goings, J.; Peng, B.; Petrone, A.; Henderson, T.; Ranasinghe, D.; Zakrzewski, V. G.; Gao, J.; Rega, N.; Zheng, G.; Liang, W.; Hada, M.; Ehara, M.; Toyota, K.; Fukuda, R.; Hasegawa, J.; Ishida, M.; Nakajima, T.; Honda, Y.; Kitao, O.; Nakai, H.; Vreven, T.; Throssell, K.; Montgomery, J. A., Jr.; Peralta, J. E.; Ogliaro, F.; Bearpark, M. J.; Heyd, J. J.; Brothers, E. N.; Kudin, K. N.; Staroverov, V. N.; Keith, T. A.; Kobayashi, R.; Normand, J.; Raghavachari, K.; Rendell, A. P.; Burant, J. C.; Iyengar, S. S.; Tomasi, J.; Cossi, M.; Millam, J. M.; Klene, M.; Adamo, C.; Cammi, R.; Ochterski, J. W.; Martin, R. L.; Morokuma,

https://doi.org/10.1021/acs.jctc.2c01315
J. Chem. Theory Comput. 2023, 19, 9102−9117

K.; Farkas, O.; Foresman, J. B.; Fox, D. J. *Gaussian 16*, revision C.01; Gaussian, Inc.: Wallingford, CT, 2016.
(69) Zhao, Y.; Peverati, R.; Yang, K. R.; Luo, S.; Yu, H. S.; He, X.; Wang, Y.; Verma, P.; Truhlar, D. G. *Minnesota-Gaussian Functional Module (MN-GFM)*, version 6.10, University of Minnesota: Minneapolis, 2018. http://comp.chem.umn.edu/mn-gfm (accessed Aug 10, 2018).
(70) Gill, P. M. W.; Johnson, B. G.; Pople, J. A.; Frisch, M. J. An Investigation of the Performance of a Hybrid of Hartree-Fock and Density Functional Theory. *Int. J. Quantum Chem.* **1992**, *44*, 319−331.
(71) Tang, K. T.; Toennies, J. P. The van der Waals Potentials Between All the Rare Gas Atoms from He to Rn. *J. Chem. Phys.* **2003**, *118*, 4976−4983.
(72) Gräfenstein, J.; Kraka, E.; Cremer, D. The Impact of the Self-Interaction Error on the Density Functional Theory Description of Dissociating Radical Cations: Ionic and Covalent Dissociation Limits. *J. Chem. Phys.* **2004**, *120*, 524−539.
(73) Lundberg, M.; Siegbahn, P. E. M. Quantifying the Effects of the Self-Interaction Error in DFT: When Do the Delocalized States Appear? *J. Chem. Phys.* **2005**, *122*, No. 224103.
(74) Mori-Sánchez, P.; Cohen, A. J.; Yang, W. Many-Electron Self-Interaction Error in Approximate Density Functionals. *J. Chem. Phys.* **2006**, *125*, No. 201102.
(75) Bao, J. L.; Gagliardi, L.; Truhlar, D. G. Self-Interaction Error in Density Functional Theory: An Appraisal. *J. Phys. Chem. Lett.* **2018**, *9*, 2353−2358.
(76) Slater, J. C. *Quantum Theory of Matter*, 2nd ed.; McGraw-Hill: New York, 1968; pp 333−334.

https://doi.org/10.1021/acs.jctc.2c01315
J. Chem. Theory Comput. 2023, 19, 9102−9117